ELSEVIER

Catalysis Today 28 (1996) 183–189

CATALYSIS TODAY

Surface reactions and structures of niobium oxide superfine particles

K. Obara [a,*], K. Iwasaki [a], S. Matushima [a], T. Hirose [b], M. Shioga [c], Y. Suemoto [a]

[a] *Faculty of Engineering, Kagoshima University, Korimoto 1-21-40, Kagoshima 890, Japan*
[b] *Department of Physics, College of Liberal Arts, Kagoshima University, Korimoto 1-21-40, Kagoshima 890, Japan*
[c] *Recording and Imaging Science Laboratories, Kao Corporation Haga, Tochigi 321-34, Japan*

Abstract

The surface states of niobium oxide superfine particles (NOSPs) are investigated by analyzing the pressure dependence of the dispersion of complex dielectric constants. NSOPs were formed by a magnetron sputtering system. The average size was 260 ± 25 Å. The lattice constant is $a = 3.45$ Å (bcc). NOSPs were a metastable materials which contained 50 at% oxygen. The density distributions of electric dipoles due to the surface state on the particles were obtained by approximating the data with theoretical curves. The reactivity of NSOPs was investigated on O_2, Ar and N_2. The surface reactivity of NOSPs strongly depended on the oxidation process of the niobium superfine particles. The influences of adsorption of argon were observed at the frequency regions 200 Hz $< \omega <$ 3 kHz and 400 kHz $< \omega$, where the electric dipole density increased above 0.1 Torr of argon. In N_2 gas, the anomalies of density of electric dipoles were observed at higher regions of the frequency and the gas pressure; 600 Hz $< \omega$ and $P_{N_2} > 4$ Torr, respectively.

Keywords: Surface reactions; Niobium oxide superfine particles

1. Introduction

In the view point of catalytic reactions, the density of surface states on the niobium oxides is one of the important parameters to determine the surface reactivity. Niobium–oxygen system consist of four phases; a-Nb, NbO, NbO_2 and Nb_2O_5 in equilibrium state at room temperature and, especially Nb_2O_5 has many polytypic phases [1,2].

Recently, we found the new relationships between the crystal structures of the niobium oxides with the composition of ca. 50 at% oxygen which were formed by a magnetron sputtering system [3]. At argon pressure $P_{Ar} <$ 0.2 Torr of the magnetron sputtering, thin microcrystals with five types of superlattice structures were derived. The crystal structures of all types of the superlattices were related to the cubic lattice $a_0 = 3.22$ Å. On the other hand, at $P_{Ar} > 0.3$ Torr, metastable NOSPs with a cubic lattice constant $a = 3.44$ Å (bcc) were formed. The lattice constant was related to the structures of NbO and NbO_2. These lattice constants, $a_0 = 3.22$ Å and $a = 3.44$ Å, were the prototypes at $P_{Ar} \leq 0.2$ Torr and $P_{Ar} \geq 0.3$ Torr, respectively.

These structural changes due to pressure difference depend on the density and the enthalpy

* Corresponding author.

SSDI 0920-5861(95)00225-1

of vacancies in as-grown crystals. The density of vacancies is related to the condensation rate of the crystals. In this report, we present the surface reactivities and the selectivities of the NOSPs.

2. Experimental

2.1. Preparation of niobium oxide superfine particles

NOSPs were prepared by oxidizing niobium superfine particles. The niobium superfine particles were formed at $P_{Ar} = 0.3$–0.5 Torr by using a magnetron sputtering system [4]. Fig. 1 shows the sputtering system which has an mass-speed-analyzer of the condensed niobium particles and a transfer device with electrodes for investigating the surface reaction of condensed materials without exposing the sample to air. The distributions of energy, mass and velocity of the condensed clusters were derived [5]. Fig. 2 shows a typical high resolution lattice

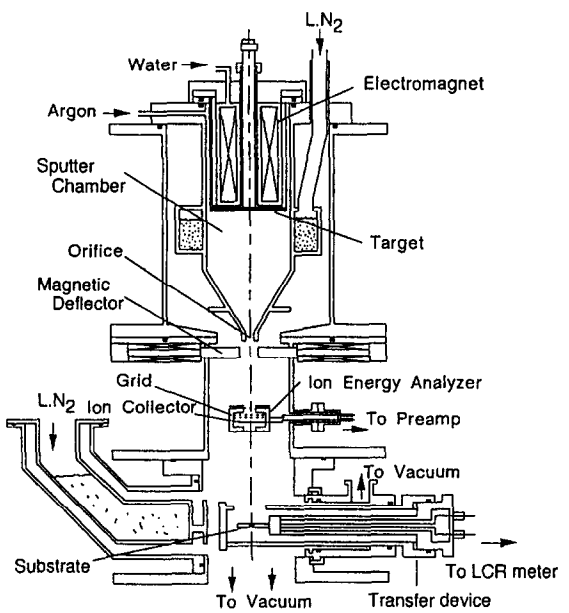

Fig. 1. Schematic diagram of the sputtering apparatus. Orifice, electromagnet, ion energy analyzer and transfer device are installed to investigate the microscopic condensation process and the surface reaction of condensed materials.

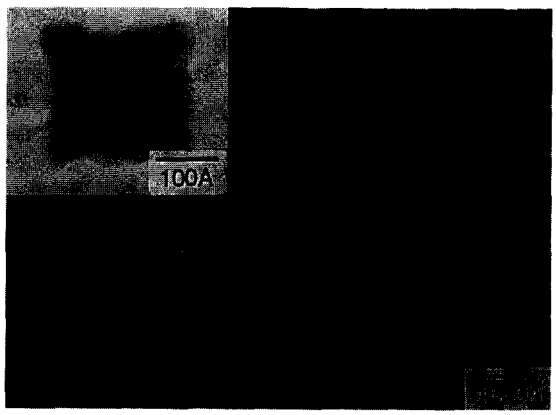

Fig. 2. High resolution electron micrograph of a niobium oxide super-fine particle. Lattice constant is $a = 3.40$ Å.

image of a NOSP after being exposed to air. The NOSP shows rough (100) surfaces and the small region with different orientation due to coalescence growth. The lattice constant is $a = 3.45$ Å (bcc). The average size of NOSPs was 260 ± 25 Å. These NOSPs were a metastable material [4].

NOSPs were deposited on the area 2×4 mm^2 of sapphire substrates with four thick evaporated gold electrodes. The initial resistance of deposited NOSPs was adjusted to 300 Ω. The configuration of NOSPs is random and almost all junctions consists of a {100} lateral face of a cubic particle and an apex of another particle {111}.

2.2. Measuring system of density distribution of electric dipoles

The complex dielectric constants of the agglomerate of NOSPs were derived by measuring capacitance $C(\omega)$ and conductance $\sigma(\omega)$ by using the precision LCR meter, YHP-4284A, as follows;

$$\epsilon^* = Re(\epsilon^*) + iIm(\epsilon^*)$$
$$\propto C(\omega) - i\sigma(\omega)/\omega \qquad (1)$$

where ω is the frequency of applied electric field. Measurements were done under a constant voltage 1 V. The complex dielectric constants of agglomerates were measured in the ranges of $10^{-7} < P < 760$ Torr and 20 Hz $< \omega <$ 1 MHz.

Each measurement of frequency dependence was continued for about 1 h repeatedly for each pressure.

The density distribution of electric dipoles (DDED) was derived from analyzing the experimental data, $C(\omega)$ and $\sigma(\omega)$, by the following relations:

$$C(\omega) = A_\infty + \sum_i^{i_{max}} 4\pi n_i e^2/m_i \times \frac{\omega_i^2 - \omega^2}{\left(\omega_i^2 - \omega^2\right)^2 + \left(\gamma_i \omega\right)^2} \quad (2)$$

$$\sigma(\omega) = \sum_i^{i_{max}} 4\pi n_i e^2/m_i \frac{\gamma_i \omega^2}{\left(\omega_i^2 - \omega^2\right)^2 + \left(\gamma_i \omega\right)^2} \quad (3)$$

where n_i is the density of ith dipoles with equivalent mass m_i, negative charge e, their natural angular frequency of oscillation ω_i and damping constant γ_i. i_{max} is the maximum index for ω_i derived from experimental data and A_∞ is the contribution from the dipoles with $i > i_{max}$ ($\omega_{i+1} > \omega_i$).

In applying Eqs. (2) and (3) to the experimental data, all data for ω_i, γ_i and n_i must be given. We assumed the following assumptions about ω_i, γ_i and n_i [6]:

(1) a group of $\{\omega_i\}$ forms a power series,

(2) γ_i is proportional to ω_i,

(3) n_i is roughly proportional to ω_i and finally adjusted so that the calculated $C(\omega)$ fits the experimental data.

If n_i is proportional to ω_i, the calculated curve becomes a flat line. This feature is a favorable characteristic for the back ground of DDED.

3. Results

3.1. Oxidation process of niobium superfine particles

Oxidation procedure strongly influences the surface reactivity of NOSPs. When the niobium

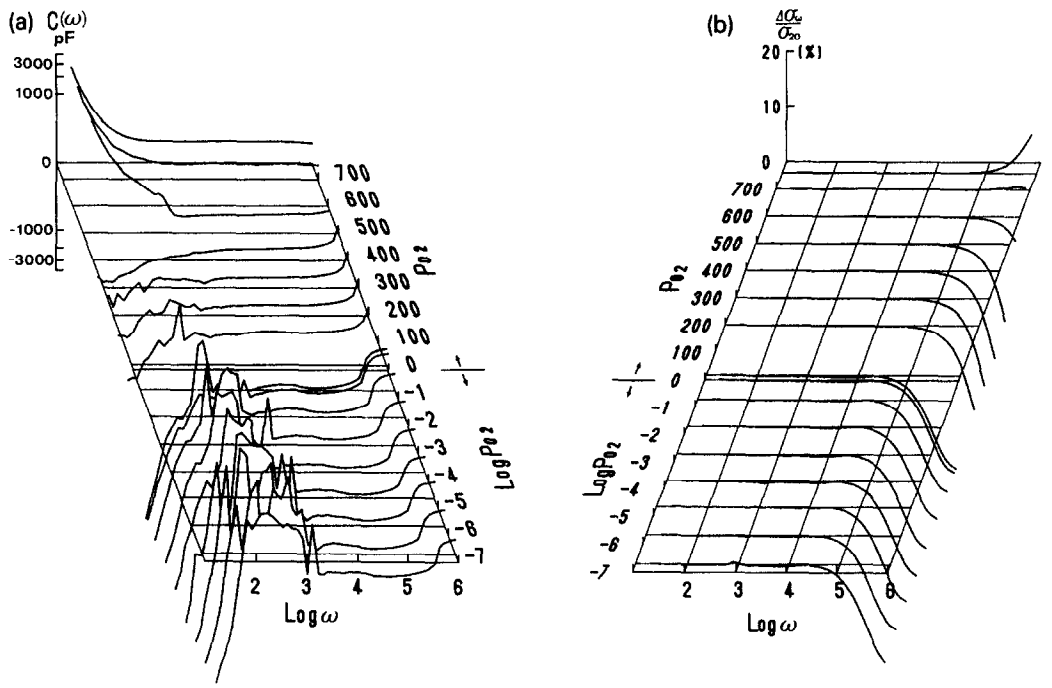

Fig. 3. (a) P_{O_2} dependences of $C(\omega)$ and $\Delta\sigma_\omega/\sigma_{20}$ of agglomerations of superfine particles. $C(\omega)$ can be classified into three regions; $P_{O_2} < 10$ Torr, $10 < P_{O_2} < 500$ Torr and $500 < P_{O_2} < 760$ Torr. (b) The pressure dependences of $\Delta\sigma_\omega/\sigma_{20}$ are well correlated with $C(\omega)$ in the high frequency region.

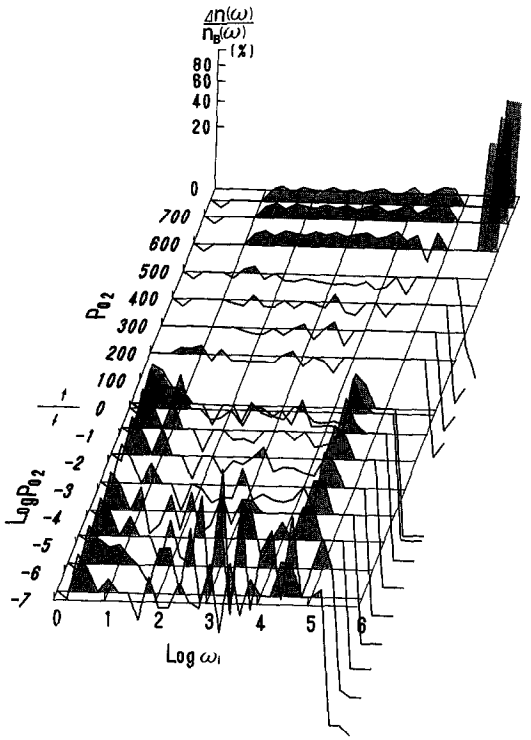

Fig. 4. P_{O_2} dependence of $\Delta n(\omega)/n_B(\omega)$. DDEDs shift to the high frequency side at 10^{-3} Torr, 10 Torr and 500 Torr.

superfine particles were gradually oxidized, $C(\omega)$ and $\sigma(\omega)$ of NOSPs showed a reversible characteristic for the change of pressure as shown in Fig. 3a and b. In this case, each measurement of frequency dependence was continued for 1.5 h repeatedly for each oxygen pressure. On the other hand, after a rapid oxidation, NOSPs hardly depended on the oxygen pressure and showed the same characteristic as that at the high oxygen pressure $P_{O_2} > 600$ Torr in Fig. 3.

Frequency dependence of $C(\omega)$ and $\sigma(\omega)$ in Fig. 3a and b can be classified into three regions; (1) in $\omega < 1$ kHz, $C(\omega)$ strongly depended on the oxygen pressure, (2) in 1 kHz $< \omega < 300$ kHz, $C(\omega)$ became negative, (3) in $\omega > 500$ kHz, $\sigma(\omega)$ strongly depended on the frequency. $C(\omega)$ and $\sigma(\omega)$ increased stepwise at 10 Torr and 600 Torr.

Fig. 4 shows the oxygen pressure dependence of DDEDs which were derived from Fig. 3a and b. To show clearly the quantities adjusted for fitting, the vertical axis is plotted by $\Delta n(\omega)/n_B(\omega)$, where $\Delta n(\omega) = n(\omega) - n_B(\omega)$. $n(\omega)$ and $n_B(\omega)$ are DDED and the flat-background distribution, respectively. Oxygen pressure dependence of DDEDs changed critically at $P_{O_2} = 10^{-3}$ Torr, 10 Torr and 600 Torr. The changes of DDED in 100 Hz $< \omega <$ 10 kHz at $P_{O_2} < 10^{-3}$ Torr are due to the small change of $C(\omega)$. The change of DDEDs at 10 Torr shows the disappearances of dipoles at 2 Hz $< \omega <$ 10 Hz and 20 kHz $< \omega <$ 80 kHz and the generation of the dipoles at 200 kHz $< \omega <$ 500 kHz. In $P_{O_2} > 600$ Torr, the increases of the density of dipoles are observed in the wide range of frequency 10 Hz $< \omega$ and, especially, an sharp increases of DDEDs are observed above 500 kHz. The features of DDEDs well agree with those of the dispersion of the capacitance. Therefore, we consider only the dispersion of the capacitance for each experiment.

3.2. Argon pressure dependence of DDEDs of NOSPs

Fig. 5 shows the argon pressure dependence of the dispersion of NOSPs. NOSPs in this experiment were formed in the rapid oxidation procedure. The pressure dependence of $C(\omega)$ is small except for the regions 200 Hz $< \omega <$ 2 kHz and 200 kHz $< \omega$. $C(\omega)$ in 200 Hz $< \omega <$ 2 kHz complexly depends on the frequency and gradually increases as P_{Ar} increases. The background of $C(\omega)$ slightly increased stepwise at $P_{O_2} = 10^{-2}$ Torr and $P_{O_2} = 4$ Torr. $C(\omega)$ at $\omega > 200$ kHz decreased suddenly in 0.05 Torr $< P_{O_2} <$ 1 Torr as shown by the arrow in Fig. 5. These characteristics were reversible to the change of the argon pressure.

Fig. 6 shows the argon pressure dependence of DDEDs which were derived from $C(\omega)$ in Fig. 3. The large increases of $\Delta n(\omega)/n_B(\omega)$ were observed in 20 Hz $< \omega <$ 100 Hz and 100 kHz $< \omega$ above 0.05 Torr of argon. Especially, the increase of $\Delta n(\omega)/n_B(\omega)$ above 200 kHz was several times the background distribution,

which suggests the large amount of argon adsorption. In 100 Hz < ω < 10 kHz, the periodic structures of DDEDs were observed above 0.05 Torr of argon. The periodic structures in DDEDs are related to the step or peak type characteristics in $C(\omega)$. The change from the monotonic characteristics to the periodic one suggests the reconstruction of the surface dipole moments induced by the argon atoms.

3.3. Nitrogen pressure dependence of DDEDs of NOSPs

To check the reactivity of NOSPs, nitrogen pressure dependence of $C(\omega)$ and $\sigma(\omega)$ were measured in the range of $P_{N_2} > 0.01$ Torr on the same sample of the experiment on argon gas. Fig. 7 shows N_2 dependence of $C(\omega)$. The background capacitance in low pressure was 13 pF, which was the same value as that in the case of argon gas. Dips of $C(\omega)$ in 100 Hz < ω < 1 kHz were smaller than those in Fig. 5 and did not become negative. The N_2 pressure dependence of $C(\omega)$ below 10 kHz were qualitatively similar to that in Fig. 5, but the magnitude of the frequency dependence was smaller than that of the case of argon. The decreases of $C(\omega)$ above 200 kHz, which showed the same characteristics at 0.005 Torr < P_{Ar} < 0.1 Torr in Fig. 5, have the similar characteristic to each other except for the increase of the frequency-independent term at $P_{N_2} > 40$ Torr.

Figure 8 shows a N_2 pressure dependence of $\Delta n(\omega)/n_B(\omega)$. The periodic characteristics as a function of frequency exist in the whole region of the pressure of nitrogen. The changes of the periodicity of $\Delta n(\omega)/n_B(\omega)$ were observed at 5 Torr and 40 Torr of nitrogen. At 5 Torr, the peaks of the density of the dipoles (DOD) apparently sifted to the higher frequency side as indicated by arrows. The increase of the frequency-independent capacitance at 40 Torr referred to the increase of DODs at 50 kHz and the decrease of that at 80 kHz. The decrease of $C(\omega)$ at $\omega > 200$ kHz below 100 Torr of nitrogen referred to the increase of DOD at ca. 100 kHz and the decrease of DOD at ca. 300 kHz from the background distribution. $C(\omega)$ and DDEDs of NOSPs were not reversible to the change of N_2 pressure.

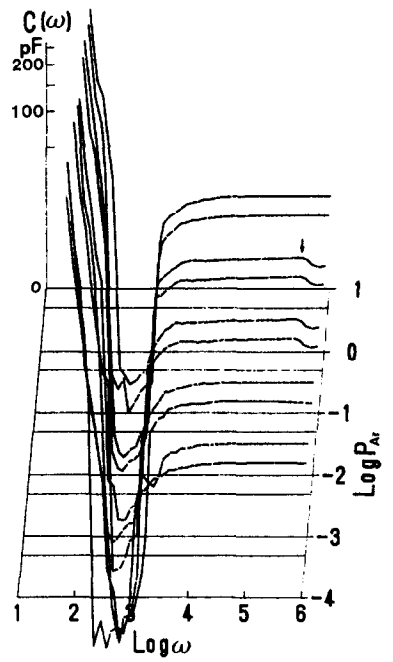

Fig. 5. P_{Ar} dependences of $C(\omega)$. NOSPs were prepared by the gradual oxidation procedure. $C(\omega)$ was plotted as $C^{1/3}$. $C(\omega)$ changed as ω^{-2} below 300 Hz. In 200 Hz < ω < 1 kHz, $C(\omega)$ became negative.

4. Discussion

The surface states of the oxide are responsible to the electric field on the surface. The changes of the surface charge and the charge in the surface states can be presented as differential capacitance $C_0 = \beta|\partial Q/\partial V_s| = C_{sc} + C_s$, where β is a constant due to the geometrical factors, Q is the induced charge by the surface potential V_s, C_{sc} and C_s are the capacitance due to the space charge and the surface states, respectively [7].

$C(\omega)$ of AC capacitance techniques represents the ensemble of the dipoles of many types under the applied surface potential. In the present case, the amplitude of V_s was estimated as 10 μV for each junction from the average size

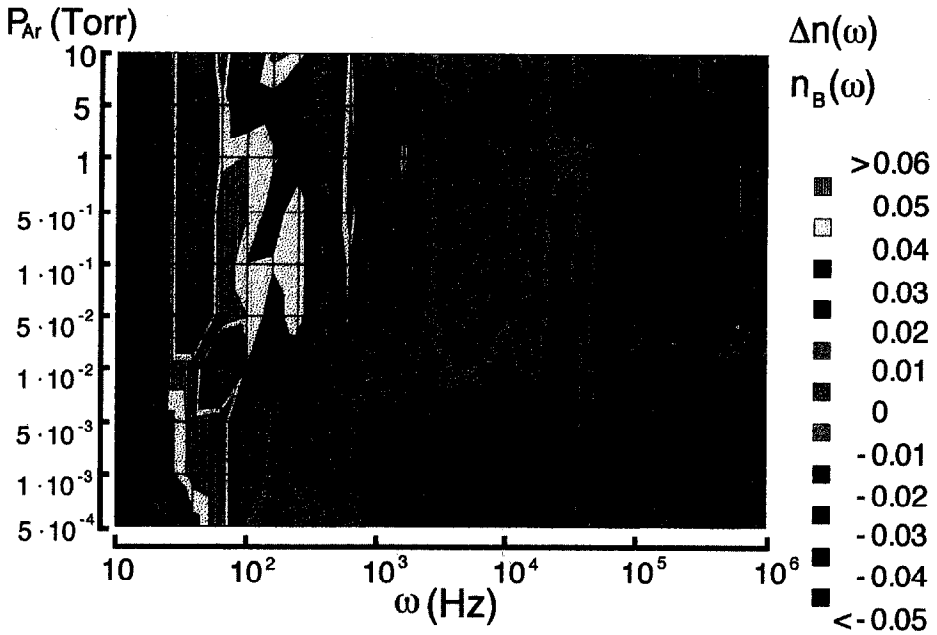

Fig. 6

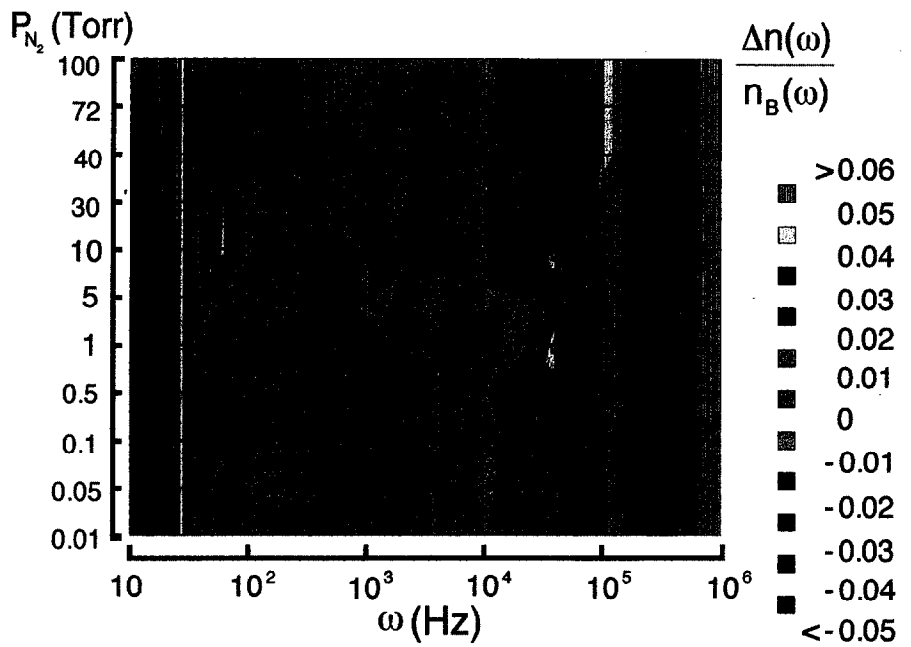

Fig. 8

Fig. 6. P_{Ar} dependences of $\Delta n(\omega)/n_B(\omega)$. The vertical axis is a conventional axis which is not proportional to the values of log P_{Ar}. Note the changes of pattern at 0.01 Torr and 5 Torr.

Fig. 8. P_{N_2} dependences of $\Delta n(\omega)/n_B(\omega)$. the vertical axis is a conventional axis which is not proportional to the values of log P_{N_2}. Note the changes of pattern at 5 Torr and 40 Torr.

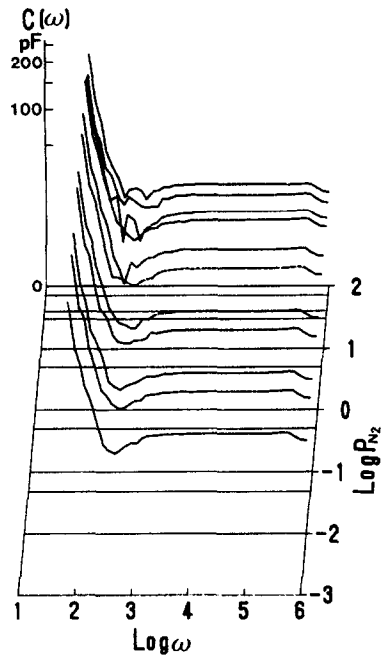

Fig. 7. P_{N_2} dependences of $C(\omega)$. NOSPs were the same sample in the case of the experiment of argon gas. $C(\omega)$ was plotted as $C^{1/3}$. $C(\omega)$ changed as ω^{-2} below 300 Hz. The change of $C(\omega)$ is smaller than that of argon gas.

of NOSPs and the applied voltage 1 V. Therefore, the presented result, $C(\omega)$ and DDEDs show the dispersion of the dipoles which exist near the Fermi energy.

The selectivities of NOSPs for O_2, Ar and N_2 are summarized as follows:

(1) *Oxygen*: the selectivity depended on the oxidation procedure of the niobium superfine particles. In the kinetics of growth of oxide on niobium superfine particles showed critical change of the growth rate at $P_{O_2} = 10^{-3}$ Torr [8]. P_{O_2} dependence of growth rates changed near $P_{O_2} \sim 10^{-3}$ Torr from $P_{O_2}^{1/2}$ to $P_{O_2}^{1/4}$, which suggested the formation of neutral defect clusters $[O_i''(M_{Nb}^{\cdot})_2]^x$ and monovalent defect clusters $[O_i''M_{Nb}^{\cdot}]'$, respectively. The slow-oxidation procedure forms metastable surface oxides. The difference of the structure formed on the surface causes the scattering of the characteristics. The critical P_{O_2} values of $C(\omega)$ and DDEDs were observed at 10^{-3} Torr, 10 Torr and 600 Torr. DDEDs shifted to the high frequency region as P_{O_2} pressure increased.

(2) *Argon*: the NOSPs were formed by the rapid oxidation procedure. The argon pressure dependence of $C(\omega)$ was small and reversible. The critical P_{Ar} values of $C(\omega)$ and DDEDs were observed at 0.05 Torr and 4 Torr. DDEDs showed periodic structures above 0.01 Torr.

(3) *Nitrogen*: the NOSPs were the same sample in the case of argon. The critical P_{N_2} pressures of $C(\omega)$ and DDEDs were observed at 5 Torr and 40 Torr. The periodic pattern shifted to the higher frequency side at 5 Torr and the magnitudes of the periodic structures of DDEDs in 10 kHz $< \omega <$ 200 kHz were increased above 40 Torr of nitrogen. The background of $C(\omega)$ was not reversible to the change of N_2 pressure. The irreversibility of $C(\omega)$ suggests the chemical bonds with higher ω_i, which contribute the back ground of $C(\omega)$ in low frequency.

5. Conclusion

The surface states of NOSPs were investigated by the AC capacitance technique. From analyzing the dispersion of the capacitance, the density distribution of electric dipoles were derived. DDEDs showed the quantitative changes of the selectivity and the reactivity as the changes of the critical pressures and the pattern of DDEDs due to the change of gas.

References

[1] N. Terao, Jpn. J. Appl. Phys., 2 (1963) 156.
[2] A.M. Samarin (Ed.), Alloys of Niobium, Israel Program for Sci. Trans., Jerusalem, 1965, p. 79.
[3] K. Obara, J. Crystal Growth, 128 (1993) 1166.
[4] K. Obara, Nucl. Instrum. Meth., B59/60 (1991) 211.
[5] K. Obara, J. Crystal Growth, 128 (1993) 262.
[6] K. Obara, M. Shioga and T. Hirose, Surf. Sci., 283 (1993) 387.
[7] V.F. Kiselevand and O.V. Krylov, Electronic Phenomena in Adsorption and Catalysis, Springer-Verlag, New York, 1987.
[8] K. Obara, K. Minami and T. Hirose, J. Crystal Growth, 99 (1990) 192.